

# Faraday Discussions

Accepted Manuscript



This manuscript will be presented and discussed at a forthcoming Faraday Discussion meeting. All delegates can contribute to the discussion which will be included in the final volume.

**Register now to attend!** Full details of all upcoming meetings: <http://rsc.li/fd-upcoming-meetings>



This is an *Accepted Manuscript*, which has been through the Royal Society of Chemistry peer review process and has been accepted for publication.

*Accepted Manuscripts* are published online shortly after acceptance, before technical editing, formatting and proof reading. Using this free service, authors can make their results available to the community, in citable form, before we publish the edited article. We will replace this *Accepted Manuscript* with the edited and formatted *Advance Article* as soon as it is available.

You can find more information about *Accepted Manuscripts* in the [Information for Authors](#).

Please note that technical editing may introduce minor changes to the text and/or graphics, which may alter content. The journal's standard [Terms & Conditions](#) and the [Ethical guidelines](#) still apply. In no event shall the Royal Society of Chemistry be held responsible for any errors or omissions in this *Accepted Manuscript* or any consequences arising from the use of any information it contains.



Journal Name

ARTICLE

## 2D-patterning of self-assembled silver nanoisland films

Semen Chervinskii<sup>\*a,b</sup>, Igor Reduto<sup>c</sup>, Alexander Kamenskii<sup>b</sup>, Ivan S. Mukhin<sup>c,d</sup> and Andrey A. Lipovskii<sup>b,c</sup>

Received 00th January 20xx,  
Accepted 00th January 20xx

DOI: 10.1039/x0xx00000x

www.rsc.org/

The paper is dedicated to recently developed by the authors technique of silver nanoislands growth, allowing self-arrangement of 2D-patterns of the nanoislands. The technique employs silver out-diffusion from ion-exchanged glass in the course of annealing in hydrogen. To modify the silver ions distribution in the exchanged soda-lime glass we included the thermal poling of the ion-exchanged glass with a profiled electrode as an intermediate stage of the processing. Resulting consequence consists of three steps: i) during the ion exchange of the glass in  $\text{Ag}_x\text{Na}_{1-x}\text{NO}_3$  ( $x=0.01-0.15$ ) melt we enrich subsurface layer of the glass with silver ions; ii) under the thermal poling, electric field displaces these ions deeper in the glass under 2D profiled anodic electrode, the displacement is smaller under hollows in the electrode where the intensity of the field is minimal; iii) annealing in reducing atmosphere of hydrogen results in silver out-diffusion only in the regions corresponded to the electrode hollows, as a result silver forms nanoislands following the shape of the electrode. Varying the electrode and mode of the processing allows governing nanoislands size distribution and self-arrangement of isolated single nanoislands, couples, triples or groups of several nanoislands—so-called plasmonic molecules.

### Introduction

Plasmonic nanostructures have recently attracted essential attention due to their perspectives for applications employing light-matter interaction. Silver, copper and gold nanoparticles, their complexes, and various nanostructures of these materials demonstrate surface plasmon resonance (SPR) in visible spectral range and, respectively, essential enhancement of local electric field under irradiation with resonant wavelength [1]. These resonant properties were employed in surface-enhanced Raman spectroscopy [2], biosensing [3], light emission and fluorescence enhancement [4-5], catalysis, photovoltaics and solar cells [6-8]. The wavelength of the SPR depends on material, geometry and size of a nanostructure as well as on dielectric permittivity of its environment. Particular interest was related to different ways of arrangement of plasmonic nanostructures from separate nanoparticles [9-11]. Control over shape, size of the nanoparticles and their interaction allows governing resonant properties of the whole nanostructure [12-13]. For example, placing plasmonic nanoparticles with small gaps between them allows achieving extremely high electric field intensity in these narrowings at the SPR wavelength [12]. At the same time, single nanoparticles are promising for sensing as their characteristics can be affected by analytes even more drastically than ones of

their complexes [14-16]. Formation of intrinsically disordered self-assembled nanostructures also corresponds to arising interest to resonant properties of disordered media [17-19].

To fabricate separated nanoparticles chemical [20] or, since recently, laser ablation and other techniques [21,22] are in use. Also, different sputtering techniques combined with thermal annealing are standard in manufacturing of metal island films (MIFs) [23,24] that are ensembles of metal nanoislands, i.e. nanoparticles. Fabrication of groups of nanoparticles is usually based on deposition of metal film and nanostructuring of this film using lithographic, preferably electron or nanoimprint lithography, processing [25,26]. Other techniques include constructing of plasmonic structures from commercially available nanoparticles using lithographic or organic templates [27,28]. Processing of MIF with lithographic techniques could be a good candidate to make given groups of nanoparticles the faster way, however fragility of MIFs does not allow this.

Recently we have developed plasmonic nanoparticles growth technique based on out-diffusion of metals from ion-exchanged glasses in the course of their annealing in reducing atmosphere [29]. The advantages of this technique are its easiness and thus cheapness, since it can be performed using very simple equipment. Ion exchange is well-known method to enrich subsurface layer of a glass with metal ions from molten salt of the metal via replacement of initial alkali ions of the glass [30]. After that these ions are subjected to reduction, for that we heat up the samples in reducing (hydrogen) atmosphere, reduced atoms then clusterize and can form nanoparticles either on the glass surface (MIF) or in the subsurface layer of the glass (glass-metal nanocomposite, GMN) [31,32].

<sup>a</sup> University of Eastern Finland, P.O.Box 111, Joensuu, 80101 Finland.

<sup>b</sup> Peter the Great St. Petersburg Polytechnic University, 29 Polytechnicheskaya, St. Petersburg, 195251 Russia.

<sup>c</sup> St. Petersburg Academic University, 8/3 Khlopina, St. Petersburg, 194021 Russia.

<sup>d</sup> ITMO University, 49 Kronverksky, St. Petersburg, 197101 Russia

\* E-mail: semen.chervinskii@uef.fi, semen.chervinsky@gmail.com

In this paper, we discuss our latest results on growth of 2D-patterned silver nanoisland film that is the ensemble of small groups of nanoislands. To provide the 2D-patterning we employed adjustment of silver ions distribution in the glass after ion exchange. For that we used thermal poling (heat treatment under DC electrical field) of ion-exchanged glasses with profiled in submicron scale anodic electrode. Resulting structures of silver nanoislands followed the shape of the electrode surface. We demonstrated that depending on this shape and processing conditions it is possible to obtain a variety of nanostructures, from areas filled with randomly distributed nanoislands to single nanoislands and groups of two, three or more nanoislands (“plasmonic molecules”).

## Experimental

### Ion exchange

We used commercially available Menzel soda-lime glass slides with composition shown in Table 1 [33]. The pre-cleaned with acetone slides of 1.0 x 26 x 76 mm<sup>3</sup> were subjected to silver-sodium ion exchange in Ag<sub>x</sub>Na<sub>1-x</sub>NO<sub>3</sub> (x=0.01..0.15) melt at temperature of 325 °C for time from 5 minutes to an hour (Fig. 1-I). For better uniformity of the processing the samples were periodically shaken to avoid formation of bubbles on the glass surface resulting from minor decomposition of the melt. During this step silver ions from the melt replaced sodium ions of the glass that resulted in silver-enriched layers under immersed surfaces of the glass. Final ion distribution in such a layer depends on properties of the glass, silver concentration in initial melt, ion exchange temperature, and duration [34]. Under typical conditions of x=0.05 and 20 min duration of the ion exchange at 325°C, about 50 % of sodium ions at the glass surface were replaced with silver ones, the descending concentration profile of which decayed by the depth of 10 microns with 50% concentration level corresponding to 5 microns distance from the surface [35]. These conditions of ion exchange are default for the experiments presented in this paper, if other is not stated.

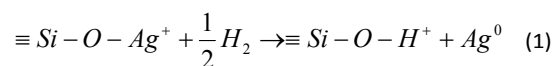
Table 1. Menzel glass chemical composition, wt.% [33].

Silicon Dioxide	SiO <sub>2</sub>	72.20%
Sodium Oxide	Na <sub>2</sub> O	14.30%
Potassium Oxide	K <sub>2</sub> O	1.20%
Calcium Oxide	CaO	6.40%
Magnesium Oxide	MgO	4.30%
Aluminium Oxide	Al <sub>2</sub> O <sub>3</sub>	1.20%
Ferric Oxide	Fe <sub>2</sub> O <sub>3</sub>	0.03%
Sulfur Trioxide	SO <sub>3</sub>	0.30%

### Annealing

Ion exchanged glasses were annealed in reducing atmosphere (mainly hydrogen, but air was also employed) at 75-350 °C for time from 30 seconds to 3 hours (Fig. 1-II). During this step hydrogen (in case of air it comes from water vapors decomposition at the glass surface [36]) diffuses into subsurface region of the glass and reduces silver ions to

neutral atoms via replacing silver in the bonds with nonbridging oxygen [37]:



The reduction results in the formation of solid solution of neutral silver in the glass matrix, which tends to decompose because of low solubility of atomic silver in glasses. The decomposition provides the formation of silver clusters and nanoparticles, in particular, silver self-assembled nanoisland film, on the glass surface, which is a strong sink for silver atoms [32]. These out-diffused nanoisland films have demonstrated applicability in surface enhanced Raman scattering [37,38]. Generally, the described above can be employed to grow nanoparticles of all noble metals. In other experiments, we used this for the formation of copper nanoparticles.

### Poling and annealing

To grow predetermined groups of silver nanoislands we modified silver ions distribution in the glass by thermal poling [39] of the ion-exchanged glass slides with profiled anodic electrode with submicron hollows in the surface. The electrode was manufactured using electron lithography followed by ion etching, as described in the next section, while nickel cathodic electrode was flat. DC voltage applied for the poling was of 500-600 V. The poling was performed at temperatures of 200-350 °C for time from 30 seconds to 30 minutes; in some cases preheating for several minutes before applying the DC field was used. The DC field moved positively charged silver ions under the positive electrode deeper in the glass, and the deepening under hollows in the electrode was less than under the places where the electrode was in a contact with the glass surface (Fig. 1-III). It is worth to note that this difference in deepening decreases with decreasing the size of the hollows in anodic electrode [40].

After proper annealing in hydrogen using the procedure described in previous section this modification of ions and, respectively, reduced silver distribution, controlled the out-diffusion of neutral silver. This resulted in the formation of silver nanoisland films, groups of nanoislands or isolated ones—depending on the electrode surface profiling and parameters of poling and annealing—only in the areas been under hollows in the electrode used in the poling (Fig. 1-IV). Since there are no available data on the diffusivity of silver atoms and hydrogen molecules neither in unpoled nor in poled glasses, the choice of both poling and hydrogen annealing parameters was mainly empirical one.

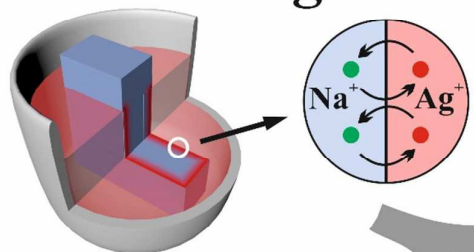
### TiO<sub>2</sub> coating

To protect silver nanoislands from contamination from the atmosphere, in some cases we coated these with amorphous TiO<sub>2</sub> layers of several nanometers in thickness using atomic layer deposition technique. TiO<sub>2</sub> was deposited at 120°C in Beneq TFS-200 reactor (Beneq, Espoo, Finland) using titanium

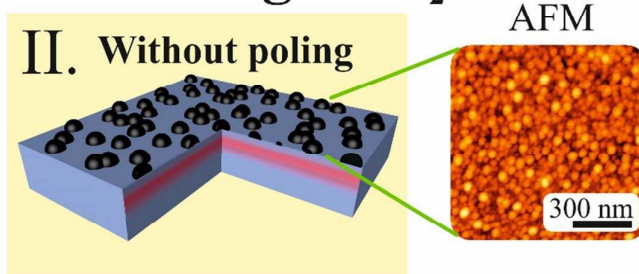
Journal Name

ARTICLE

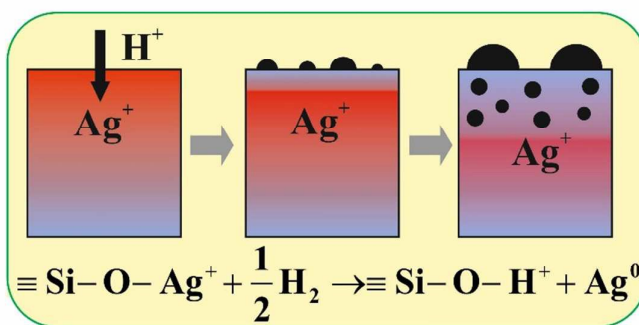
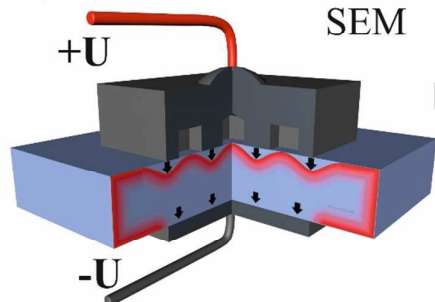
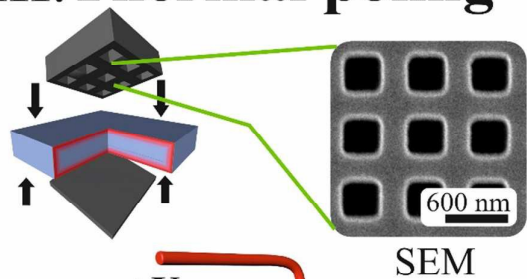
## I. Ion exchange

Annealing in H<sub>2</sub>

## II. Without poling



## III. Thermal poling



## IV. After poling

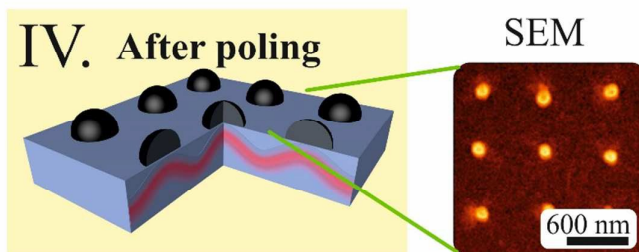


Figure 1. Schematic of the process of silver nanoisland films and structures growth. I) In ion exchange, soda-lime glass slide is immersed in  $\text{Ag}_2\text{Na}_{1-x}\text{NO}_3$  ( $x=0.01..0.15$ ) melt (325 °C, 5 minutes – hour). II) After annealing of the ion-exchanged glass slide in hydrogen atmosphere (75-350 °C, 30 seconds - 3 hours) silver nanoisland film grows. III) Thermal poling of ion-exchanged glass using profiled anode (200-350 °C, DC 500-600 V, 30 seconds - 30 minutes) allows adjustment of silver ions distribution. IV) After annealing of poled ion-exchanged glass silver nanoislands grow only where anodic electrode did not contact with the surface in poling. Inset: Hydrogen penetrating the glass reduces silver ions to atoms; in the course of diffusion and self-arrangement silver forms nanoparticles either on the glass surface or both on the surface and in the bulk of the glass.

tetrachloride ( $\text{TiCl}_4$ ) and water ( $\text{H}_2\text{O}$ ) as precursors, growth rate was 0.07 nm/cycle, between deposition cycles nitrogen was purged to remove extra precursor materials from the reactor chamber. It was also demonstrated in the experiments [37] and theoretically explained [41], that these coatings can be employed to tune surface plasmon resonance wavelength by modifying the effective dielectric permittivity of surrounding media around nanoislands due to high ( $n=2.3-3$  in a wavelengths range of 300-1300 nm) refractive index of  $\text{TiO}_2$ . In our experiments the thickness of the film varied from 3 to 100 nm.

## Electron lithography

To make profiled anode electrode from polished glassy carbon ( $R_a < 50\text{nm}$ , plates of  $3 \times 100 \times 100 \text{ mm}^3$  were obtained from Svensk Specialgratit AB and cut into pieces of  $3 \times 20 \times 25 \text{ mm}^3$ ) we employed electron beam lithography. Chromium layer of 50 nanometers was e-beam sputtered as a mask on the glassy carbon using Kurt J. Lesker Company Lab 18 thin film deposition system, after it the sample was spin-coated with electron resist, baked and exposed in Vistec Lithography Ebeam EBPG5000. Development after the exposure was performed using SSE OPTIsin SST 120 setup. The chromium

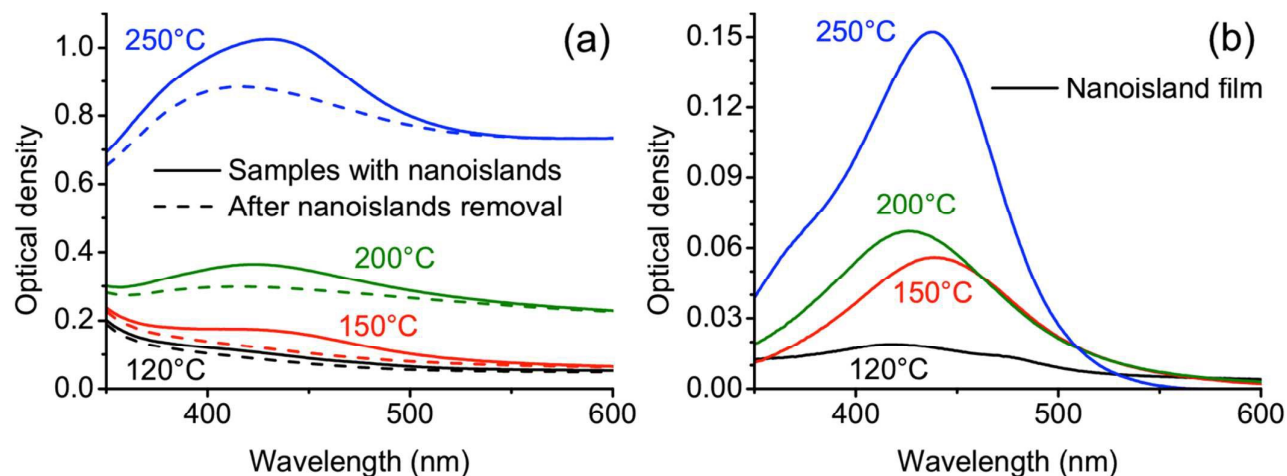


Figure 2. Spectra of samples of ion-exchanged glasses, annealed in hydrogen for 10 minutes at various temperatures (marked near the spectra) and spectra of ones after removal of grown MIF (a), and differential spectra of the nanoisland film (b).

layer was etched through developed resist in Plasmalab 100, after that finally glassy carbon was etched through chromium mask in Plasmalab 80plus. Chromium mask was then removed, and profiled glassy carbon was cleaned consequently in acetone and isopropanol using ultrasonic bath for 5-20 minutes. Resulting relief height of 50-400 nm was provided depending on the etching parameters.

#### Optical spectroscopy

To characterize optical properties of silver nanoisland films we used Specord 50 spectrophotometer, the absorption spectrum was measured firstly for the sample with MIF, after this the MIF was removed using cotton pads with acetone or isopropanol, and the spectrum was measured for the second time. The difference between these two spectra gave us the spectrum of the nanoisland film itself. Examples of measured and differential spectra are shown in Fig. 2.

#### Atomic force and electron microscopy

Structural characterization of manufactured electrodes, nanoisland films, groups and single nanoislands was performed by means of Veeco Dimension-3100 atomic force microscope with Bruker TESPA/TESP-SS tips in tapping mode and Zeiss Supra 25 scanning electron microscope. For SEM in

some cases the glass samples were coated with 10 nanometers of gold using Emitech K675X sputterer. Cross-section image of ion-exchanged glass after annealing was made using JEOL JEM 2100-F transmission electron microscope.

### Results and discussion

#### Silver nanoisland films

Using basic technique including silver ion-exchange and annealing in reducing atmosphere we succeeded in growth of metal island films consisting of silver islands from ones to tens of nanometers in size with separations of few nanometers (Fig 3). Silver nanoislands demonstrated almost hemispherical shape in AFM (Fig 4). Depending on the processing conditions, percolated and continuous films could also be grown. For the latter more silver is needed to be reduced than to obtain nanoisland film, therefore ion exchange should be performed in melt with higher concentration of silver ions, and annealing temperature and duration are also more than ones for nanoislands. We tried different annealing modes to reveal nanoislands size distribution dependencies on the processing conditions (Fig. 4). In general, nanoislands self-assembly

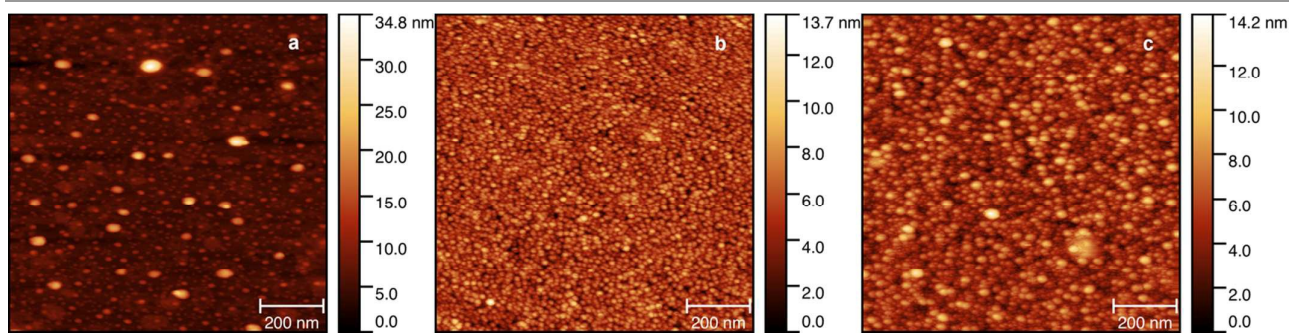


Figure 3. Silver nanoisland films grown after annealing of ion-exchanged glass at different temperatures for 10 minutes: a) 120 °C, b) 150 °C, c) 200 °C.

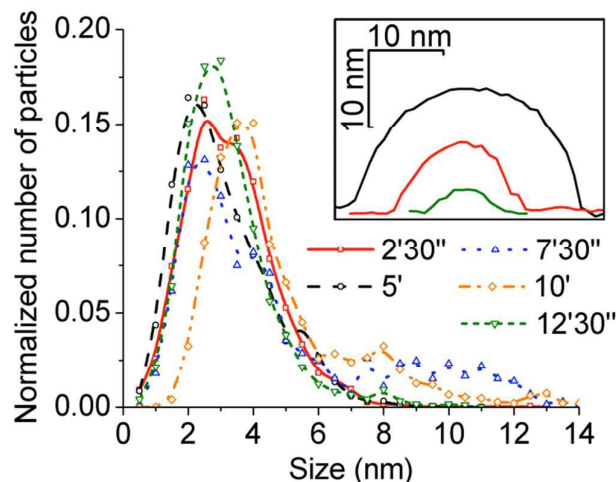


Figure 4. Size distributions of films, grown after annealing of ion-exchanged glass at 120 °C for different time from 2.5 minutes to 12.5 minutes. Inset: profiles of different nanoislands from the same sample. Reproduced with permission from [29]. Copyright 2013, AIP Publishing LLC.

occurred in agreement with recently developed model [42,43]—longer annealing as well as higher temperatures resulted in decreasing concentration and increasing the size of nanoislands [29].

We studied also the relation of optical properties of the nanoisland films and processing parameters. Predictably, absorption (intensity of surface plasmon resonance) was proportional to the amount of reduced silver, that is to the annealing duration and temperature (Fig. 2). Ion exchange parameters (duration and amount of  $\text{Ag}^+$  in the ion-exchange bath) determine silver ions distribution before annealing, therefore also affecting the film growth. However since the reduction of silver ions takes place in a layer thinner than the ion-exchanged region of the glass, duration of the ion exchange influences nanoislands formation only in case of very short durations. The same way, since almost all sodium ions near the glass surface are replaced by silver ones at  $x=0.15$  in  $\text{Ag}_x\text{Na}_{1-x}\text{NO}_3$  melt [45], less essential change in MIF formation was observed after processing of the slides in higher concentrated melts.

It should be also mentioned, that at certain annealing parameters (higher temperatures and longer times) hydrogen reduces silver deep enough to form nanoparticles in the bulk of the glass, not only surface. Typical diameter of these mostly spherical nanoparticles is below 10 nanometers (Fig. 5). Their amount also grows with the duration of hydrogen processing (compare Fig. 5a and 5b). Studies of formation and plasmonic properties of these particles are out of scope of this paper and were reported elsewhere [31,32], however, they should be

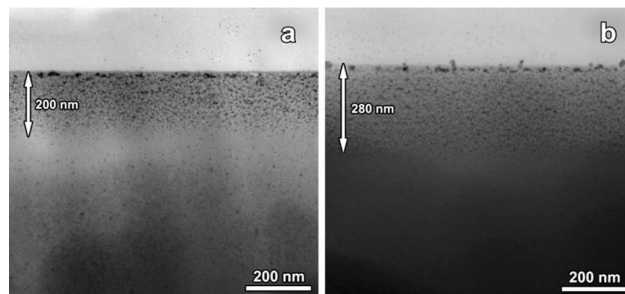


Figure 5. TEM image of silver nanoparticles, formed in ion-exchanged glass in the course of hydrogen annealing for 7.5 (a) and 15 minutes (b) at 300 °C.

taken into account in certain experiments with out-diffused silver nanoislands.

#### Poling of silver ion-exchanged glass

Spatially non-uniform thermal poling was used to adjust silver ions distribution in the glass aiming to spatially controlled growth of silver nanoislands. In poling, DC electric field moves all cations bonded before the poling to non-bridging oxygen atoms of glass network, in particular silver ions, away from anodic surface of the glass. Using this effect, we had to work out the regime, which provides deepening of silver ions sufficient to prevent nanoislands formation everywhere except desirable positions after following annealing of the poled glass slides in hydrogen. For a flat anodic electrode the deepening increases with applied voltage and duration of the poling [45-47]. Generally speaking, nanosized hollows in anodic electrode used in poling should provide spatially non-uniform electric field which is weaker under the hollows, while the maximum field intensity and thus silver ions deepening is provided between these hollows. However, it should be accounted that according to the existing model [40] lateral components of electric field generated by structured electrodes induce lateral motion of positive ions. Thus the difference of the deepening under the hollows in the anodic electrode and between the hollows is less for smaller hollows. Moreover, time dependence of this difference goes through maximum and decays for longer poling [40] that is optimal mode of the processing depends on anodic electrode topology. Precise modeling of this problem can hardly be performed because of unknown mobilities/diffusion coefficients of several species participating in the formation of the nanoislands: molecular hydrogen, neutral silver and hydronium,  $\text{H}_3\text{O}^+$ , which is the actual carrier for a hydrogen ions [44]. Moreover, since these species diffuse in poled region of glass, composition and structure of which essentially differs with ones of virgin glass

[48-49] this should modify their diffusivity in comparison with the virgin glass. The same way, since resulting 3D silver ions distribution also could hardly be directly measured, we evaluated it basing on shape and distribution of nanoislands grown after the annealing. Comparison of results on nanoislands growth obtained after poling of the ion-exchanged glasses with electrodes of different shape just confirms that although silver ions distribution follows the shape of the anodic electrode, it always smoother than the electrode rectangular shape. In general, poling mode controls silver ions deepening which either allows or forbids formation of silver nanoislands on the glass surface.

It is worth to note that the deepening results not only in a delay of silver reduction and out-diffusion because of time necessary for hydrogen to go through the silver ions depleted layer and for silver atoms to go towards the glass surface. Other effect is decreasing of silver atoms flux to the surface from bigger depths. This is because if the reduction takes place farther from the glass surface the strength of the surface sink for arisen silver atoms decreases, and the probability of out-diffusion and growth of silver nanoislands drops. Thus, the optimal poling regime should provide the sufficient difference in deepening of silver ions under the flat surface of the anodic electrode and under the hollow. This is necessary to withdraw formation of silver nanoislands in stronger poled regions between the hollows in the electrode, while the nanoislands under the hollows should grow.

#### 2D-patterned self-assembled silver nanoisland films

Using annealing of ion-exchanged glass poled with 2D-patterned electrode we succeeded in growth of structures from nanoislands, following the shape of electrode. It was demonstrated, that silver nanostructures with different distributions of nanoislands can be grown by varying poling and annealing conditions (Fig. 6), while electrode shape provides one more power of freedom to design these

nanostructures (Fig. 7). Using patterns in micron scale we obtained under the patterns the areas with nanoisland films inside quite similar to ones grown without poling, modified ions distribution influenced growth of nanoislands on the edges of these areas only. This influence resulted in bigger nanoislands on the edges of pattern, it can be explained by lower concentration of silver ions near the edges and, respectively, bigger size of critical nuclei [50]. Definitely, the same relates to nanoparticles of any material in the case of their diffusion-governed growth. The patterns with dimensions of 1  $\mu\text{m}$  and less, down to 100 nm, affected growth of nanoisland structures very much, allowing to grow nanoislands almost an order bigger then in non-patterned films, up to 150-200nm in diameter. Due to this, small hollows in electrode (300 x 300 nm<sup>2</sup> and less) allowed us to grow isolated single particles or groups of few particles—so-called plasmonic molecules—depending on processing conditions [42,43]. Figure 8 illustrates that decreasing the size of the hollows (keeping all other conditions the same) resulted not only in obvious decreasing of the number of nanoislands, but also in increasing the size of biggest islands in the “molecule”—the possible reasons of this are the difference in ion distribution at the edges of the poled areas and the decrease in the quantity of growing nanoparticles that is in their concurrence for silver atoms. It is essential that the same electrodes under different poling and annealing conditions can be used to form arrays of isolated either single nanoislands (Fig. 9) or pairs (dimers) and triples (Fig. 10). It is worth to note that by choosing proper width of the electrode hollow to fit only one particle (at certain processing conditions) self-arranged chains of nanoislands can be obtained (Fig. 11, Fig 7c). Similarly, wider elongated hollows could provide more complicated chains containing several nanoparticles placed in transverse direction. It is worth to note that all these chains possess some disordering both in longitudinal and transverse directions.

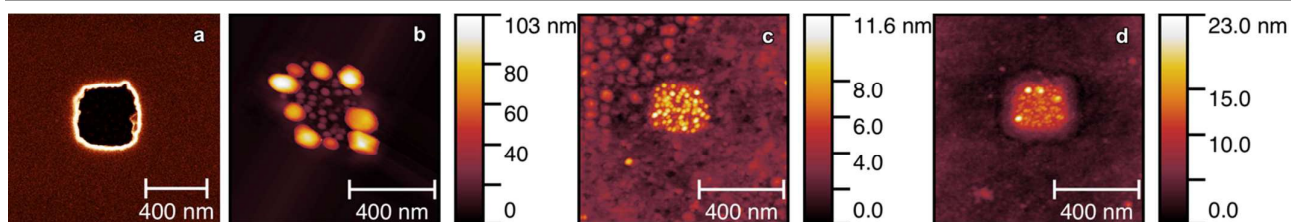


Figure 6. Electrodes with hollows of 400x400 nm<sup>2</sup> (a) and structures, grown after poling with this electrode (b-d). Ion exchanged glasses were poled with 500 V DC field at 300 °C for 60 seconds, and annealed in hydrogen for 10 minutes at 300 (b), 250 (c) and 200 °C (d).

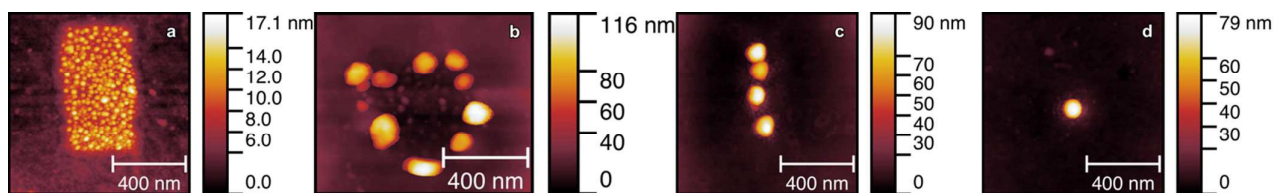


Figure 7. Examples of silver nanoisland structures obtained using developed 2D-patterning method with different electrodes, poling and annealing conditions.

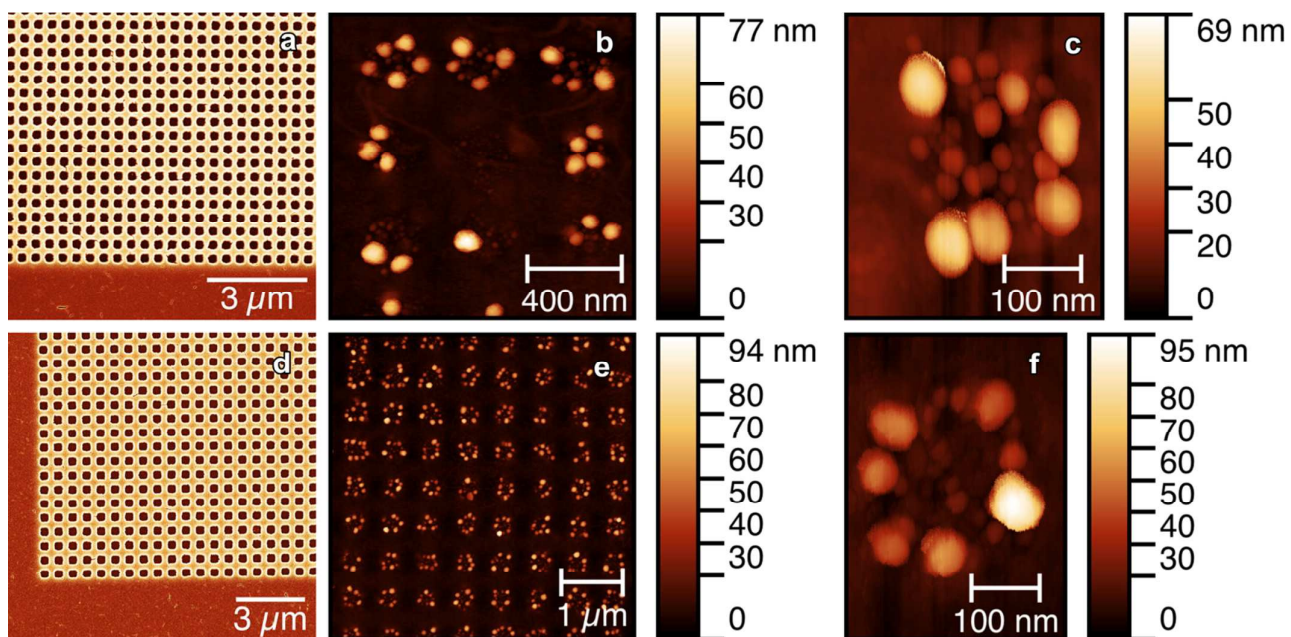


Figure 8. SEM images of the electrodes with  $200 \times 200$  (a) and  $300 \times 300$  nm<sup>2</sup> hollows (d). AFM images of silver nanostructures grown in the course of 3 minutes annealing at 315 °C, before that glass was consequently ion-exchanged and poled for 10 seconds with DC 500 V at 300 °C using these electrodes—(a) for (b, c) and (d) for (e, f), respectively.

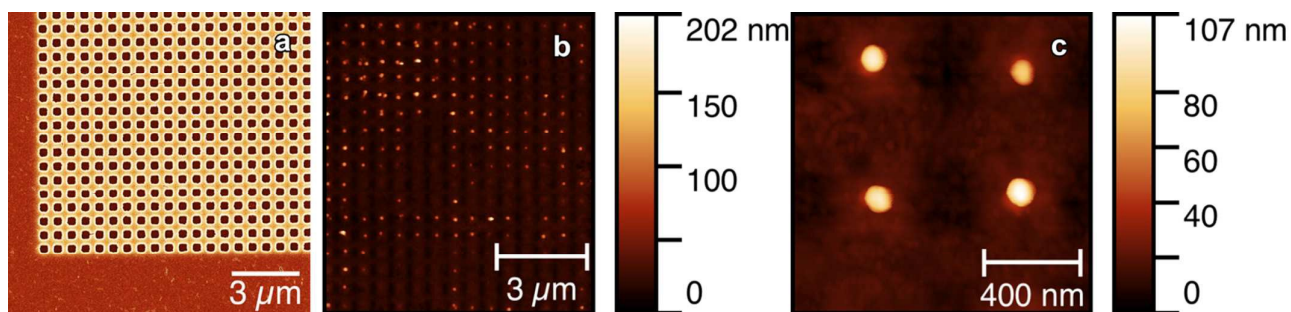


Figure 9. SEM image of the electrode with  $300 \times 300$  nm<sup>2</sup> hollows (a). AFM images of silver nanostructures (b, c) grown in the course of 5 minutes annealing at 300 °C, before that glass was consequently ion-exchanged and poled using shown in (a) electrode for 10 seconds with DC 500 V at 300 °C.

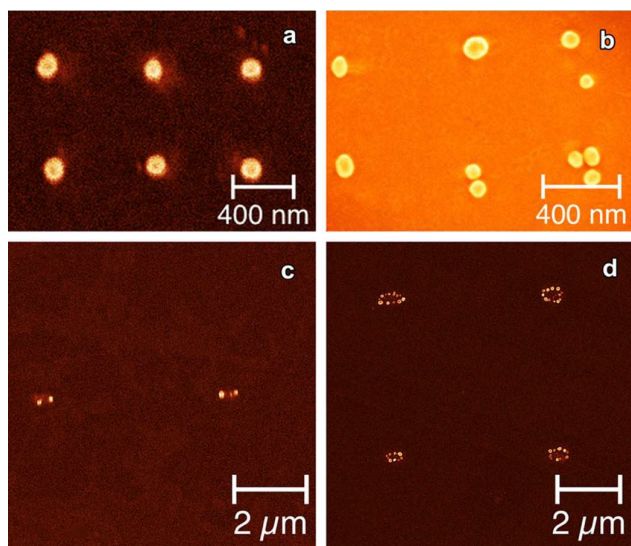


Figure 10. SEM images of silver nanostructures grown in the course of annealing for 10 minutes at 350 °C (b,e) and for 30 seconds at 300 °C (c,f), before that glass was consequently ion-exchanged and poled for 60 seconds with DC 500 V at 350 °C (b,e) and 300 °C (c,f). For (a,b) was used the electrode with  $300 \times 300$  nm<sup>2</sup> hollows, for (c,d)—with  $300 \times 600$  nm<sup>2</sup> ones.

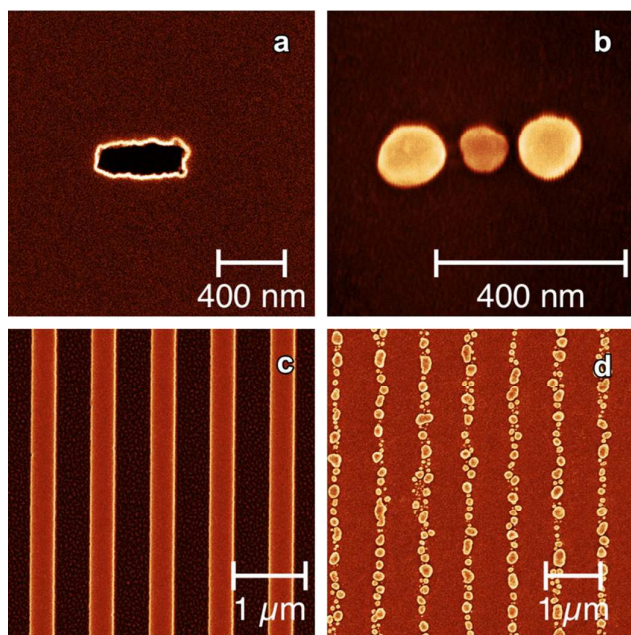


Figure 11. SEM images of the electrode with 200x600 nm<sup>2</sup> (a) and 1 μm stripe (c) hollows. SEM images of silver nanostructures grown in the course of annealing for 10 minutes (b) and for 60 seconds (d) at 300 °C, before that glass was consequently ion-exchanged and poled for 60 seconds with DC 500 V at 300 °C.

### Stability of out-diffused silver nanoislands

Although silver is known to oxidize/sulphadize in air, in case of out-diffused nanoislands these reactions did not eliminate silver, just passivated the nanoislands. We tested stability of grown nanoisland films by studying optical spectra evolution over time—spectra remained almost the same for 6 months (Fig. 12). Minor changes can, however, be explained not only by continuing degradation, but also slow reduction of silver in ion-exchanged glass even in the air at room temperature which can take place [51].

To additionally protect samples and avoid both effects in some cases we covered them with 3-5 nanometers of amorphous TiO<sub>2</sub> by means of atomic-layer deposition. Using this coating, plasmon resonance shift by 20-50 nanometers to the longer wavelengths should be taken into account. It should be noted that this shift could be less if coating material of lower refractive index, for example Al<sub>2</sub>O<sub>3</sub>, is used.

### Stability of glassy-carbon electrode

We tested different materials to make the anode and found glassy carbon to be the best option, as it is solid and does not suffer from anodic bonding (comparing to silicon, for example), can be patterned in the nanoscale, and it is commercially available with perfectly flat surface. It worth to mention that after 90 cycles of poling and cleaning etched hollows in anodic electrode enlarged only for 50 nanometers at each side that characterize the stability of the structure. However, basic cleaning technique used in the laboratory—mechanical cleaning using cotton pads with acetone—was found making minor scratches on the electrode surface as well as leaving some acetone remains affecting the contact between the electrode and glass in the poling. The best option

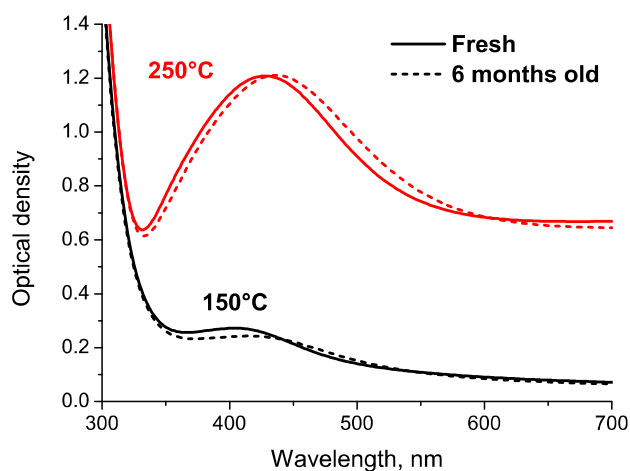


Figure 12. Optical absorption spectra of silver nanoisland films after preparation (solid) and after 6 months in the air at room temperature (dashed). Films were grown in the course of 10 minutes annealing in hydrogen at shown in the graphs temperatures.

was consequent ultrasonification in acetone and isopropanol.

### Conclusions

Finally we have designed the technique to control self-assembled growth of silver nanoislands in predefined areas of a glass surface. This is provided by thermal poling of a silver-exchanged glass with profiled anodic electrode. That allows nanoscale tuning of spatial distribution of silver ions in the subsurface region of the glass. Annealing of glasses with altered ion distribution in hydrogen results in the growth of silver nanoislands and groups of the nanoislands in less-poled areas, which correspond to hollows in the anode used in poling of the glass. Governing 3D distribution of silver ions in the glass by conditions of poling and annealing enables control of neutral silver out-diffusion. The latter allows to vary structures of nanoislands which can be self-arranged in the less-poled regions—from areas with densely placed small silver nanoislands of few nanometers in size to the arrays of single islands as big as 150-200 nm in diameter, arrays of isolated dimers and triplets of nanoislands, as well as chains and circles of the islands. It is shown that the use of glassy-carbon as anodic electrode material provides decent stability of the nanoprofiled anode on a run of tens of high voltage poling and solvent cleaning cycles. Optical properties of manufactured silver nanoislands are stable after 6 months exposure in the air. The developed technique is capable of easy fabricating differing in their spectral response structures consisting of several metal nanoislands for plasmonics and photonics applications.

### Author Contributions

S.Ch. made nanoprofiled electrodes and prepared the main part of the manuscript text. S.Ch. and I.R. developed 2D-patterning technique. S.Ch., I.R. and A.K. made samples, measured spectra, and analysed all experimental data. I.R.

drew 3D-schematic of the process. I.R. and I.S.M. performed SEM measurements. A.K. made AFM scans. A.A.L. supervised the whole work.

### Acknowledgements

The work was supported by EU (Marie Curie FP7 project #269140), Academy of Finland (grant #288151), and Russian Science Foundation (grant no. 14-22-00136). The authors thank Pavel Brunkov and Alexander Baklanov from Ioffe Institute for their help in AFM studies. S.Ch. is thankful to Janne Laukkanen, Mikhail Petrov and Denis Karpov from University of Eastern Finland for their support in electron beam lithography.

The AFM and TEM studies were performed using the equipment of the Joint Research Centre 'Material science and characterization in advanced technology' (Ioffe Institute, St. Petersburg, Russia).

### Notes and references

- 1 S. A. Maier, *Plasmonics: Fundamentals and Applications*, Springer, 2007.
- 2 Eric C. Le Ru and Pablo G. Etchegoin, *Principles of Surface-Enhanced Raman Spectroscopy*, Elsevier, 2009.
- 3 J. N. Anker, W. P. Hall, O. Lyandres, N. C. Shah, J. Zhao and R. P. van Duyne, *Nature Materials*, 2008, **7**(6) 442-53.
- 4 V. A. Podolskiy, P. Ginzburg, B. Wells and A. V. Zayats, *Faraday Discuss.*, 2015, **178**, 61-7.
- 5 M. Gaio, M. Castro-Lopez, J. Renger, N. van Hulst and R. Sapienza, *Faraday Discuss.*, 2015, **178**, 237-252.
- 6 P. Xu, L. Kang, N. H. Mack, K. S. Schanze, X. Han and H. L. Wang, *Sci. Rep.*, 2013, **3**, 2997.
- 7 C. Clavero, *Nature Photonics*, 2014, **8**, 95-103.
- 8 J. Kim, H. Choi, C. Nahm, B. Park, *Electron. Mat. Lett.*, 2012, **8**(4), 351-364.
- 9 H. Wang, D. W. Brandl, P. Nordlander and N. J. Halas, *Acc. Chem. Res.*, 2007, **40**(1), 53-62.
- 10 N. Zohar, L. Chuntonov and G. Haran, *J. Photochem. Photobiol. C*, 2014, **21**, 26-39.
- 11 C. Lee, M. Tame, J. Lim and J. Lee, *Phys. Rev. A*, 2012, **85**, 063823.
- 12 V. Klimov, *Nanoplasmonics*, Pan Stanford, 2007
- 13 R. Esteban, A. Zugarramurdi, P. Zhang, P. Nordlander, F. J. Garcia-Vidal, A. G. Borisov and J. Aizpurua, *Faraday Discuss.*, 2015, **178**, 151-183.
- 14 E. Ringe, B. Sharma, A.-I. Henry, L. D. Marks and R. P. van Duyne, *Phys. Chem. Chem. Phys.*, 2013, **15**, 4110-4129.
- 15 A. D. McFarland and R. P. van Duyne, *Nano Lett.*, 2003, **3**(8), 1057-1062.
- 16 B. de Nijs, R. W. Bowman, L. O. Herrmann, F. Benz, S. J. Barrow, J. Mertens, D. O. Sigle, R. Chikkaraddy, A. Eiden, A. Ferrari, O. A. Scherman and J. J. Baumberg, *Faraday Discuss.*, 2015, **178**, 185-183.
- 17 I. M. Lifshits, S. A. Gredeskul and L. A. Pastur, *Introduction to the theory of disordered systems*, Wiley, 1988.
- 18 V. Markel and A. Sarychev, *Phys. Rev. B*, 2007, **75**, 085426.
- 19 M. Petrov, *Phys. Rev. A*, 2014, **91**(2), 023821.
- 20 S. Panigrahi, S. Kundu, S. Ghosh, S. Nath and T. Pal, *J. Nanopart. Res.*, 2004, **6**(4), 411-414.
- 21 V. Amendola and M. Meneghetti, *Phys. Chem. Chem. Phys.*, 2009, **11**, 3805-382.
- 22 M. V. Gorokhov, V. M. Kozhevnikov, D. A. Yavsin, A. V. Ankudinov, A. A. Sitnikova and S. A. Gurevich, *Tech. Phys.*, 2012, **57**(6), 868-873.
- 23 K. Aslan, Z. Leonenko, J. R. Lakowicz and C. D. Geddes, *J. Fluoresc.*, 2005, **15**(5), 643-654.
- 24 A. Schaub, P. Slepicka, I. Kašparkova, P. Malinsky, A. Mackova and V. Švorčík, *Nanoscale Res. Lett.*, 2013, **8**, 249.
- 25 S. Madsen, P. Kempen and R. Sinclair, *Microsc. Microanal.*, 2013, **19**(2), 1554-1555.
- 26 B. Radha, S. H. Lim, M. S. M. Saifullah and G. U. Kulkarni, *Sci. Rep.*, 2013, **3**, 1078.
- 27 X. Zhang, A. V. Whitney, J. Zhao, E. M. Hicks and R. P. Van Duyne, *J. Nanosci. Nanotechnol.*, 2006, **6**, 1-15.
- 28 R. McCaffrey, H. Long, Y. Jin, A. Sanders, W. Park and W. Zhang, *J. Am. Chem. Soc.*, 2014, **136**(5), 1782-1785.
- 29 S. Chervinskii, V. Sevriuk, I. Reduto, A. Lipovskii, *J. Appl. Phys.*, 2013, **114**, 224301.
- 30 F. Gonella, *Ceram. Int.*, 2015, **41**(5), 6693-6701.
- 31 G. de Marchi, F. Caccavale, F. Gonella, G. Mattei, P. Mazzoldi, G. Battaglin and A. Quaranta, *Appl. Phys. A*, 1996, **63**(4), 403-7.
- 32 Yu. Kaganovskii, A. Lipovskii, M. Rosenbluh, V. Zhurikhina, *J. Non-Cryst. Solids*, 2007, **353**, 2263-2271.
- 33 Menzel-Glaser: Microscope slides (Accessed 22.08.2015) <http://menzel.de/Microscope-Slides.687.0.html?&L=1>
- 34 J. Linares, D. Sotelo, A. A. Lipovskii, V. V. Zhurikhina, D. K. Tagantsev, J. Turunen, *Opt. Mat.*, 2000, **14**(2), 145-153.
- 35 V. V. Zhurikhina, M. I. Petrov, K. S. Sokolov, O. V. Shustova, *Tech. Phys.*, 2010, **55**(10), 1447-1452
- 36 P. L. Inácio, B. J. Barreto, F. Horowitz, R. R. B. Correia and M. B. Pereira, *Opt. Mat. Express*, 2013, **3**(3), 390-399.
- 37 S. Chervinskii, A. Matikainen, A. Dergachev, A. Lipovskii and S. Honkanen, *Nanoscale Res. Lett.*, 2014, **9**, 398.
- 38 V. V. Zhurikhina, P. N. Brunkov, V. G. Melehin, T. Kaplas, Yu. Svirko, V. V. Rutckaia, A. A. Lipovskii, *Nanoscale Res. Lett.*, 2012, **7**, 676.
- 39 C. M. Lepienski, J. A. Giacometti, G. F. L. Ferreira, F. L. Freire and C. A. Achete, *J. Non-Cryst. Solids*, 1993, **159**(3), 204-212.
- 40 K. Sokolov, V. Melehin, M. Petrov, V. Zhurikhina and A. Lipovskii, *J. Appl. Phys.*, 2012, **111**(10), 104307.
- 41 S. A. Scherbak, O. V. Shustova, V. V. Zhurikhina and A. A. Lipovskii, *Plasmonics*, 2015, **10**(3), 519-527.
- 42 A. Redkov, S. Chervinskii, A. Baklanov, I. Reduto, V. Zhurikhina and A. Lipovskii, *Nanoscale Res. Lett.*, 2014, **9**, 606.
- 43 A. Redkov, S. Chervinskii, A. Baklanov, I. Reduto, V. Zhurikhina and A. Lipovskii, *Nanoscale Res. Lett.*, 2015, **10**, 201.
- 44 V. V. Zhurikhina, M. I. Petrov, K. S. Sokolov and O. V. Shustova, *Tech. Phys.*, 2010, **55**(10), 1447-1452.
- 45 R. H. Doremus, *Appl. Phys. Lett.*, 2005, **87**, 232904.
- 46 A. A. Lipovskii, V. V. Rusan and D. K. Tagantsev, *Solid State Ionics*, 2010, **181**(17-18), 849-855.
- 47 M. I. Petrov, A. V. Omelchenko and A. A. Lipovskii, *J. Appl. Phys.*, 2011, **109**(9), 094108.
- 48 M. Dussauze, V. Rodriguez, A. Lipovskii, M. Petrov, C. Smith, K. Richardson, T. Cardinal, E. Fargin and E. I. Kamitsos, *J. Phys. Chem. C*, 2010, **114**(29), 12754-12759.
- 49 A. V. Redkov, V. G. Melehin and A. A. Lipovskii, *J. Phys. Chem. C*, 2015, **119**(30), 17298-17307.
- 50 A. V. Redkov, A. A. Lipovskii and V. V. Zhurikhina, *J. Non-Cryst. Solids*, 2013, **376**, 152-157.
- 51 I. Reduto, S. Chervinskii, A. Matikainen, A. Baklanov, A. Kamenski and A. Lipovskii, *J. Phys.: Conf. Ser.*, 2014, **541**, 012073.